

THE METHOD OF FUNDAMENTAL SOLUTIONS FOR STATIONARY FLOW THROUGH AN AXISYMMETRIC CYLINDRICAL FIBROUS FILTER

JAN ADAM KOŁODZIEJ, PAWEŁ FRITZKOWSKI

Poznan University of Technology, Institute of Applied Mechanics, Poznań, Poland

e-mail: jan.kolodziej@put.poznan.pl; pawel.fritzkowski@gmail.com

A problem of steady-state incompressible fluid flow through a fibrous cylindrical filter is considered. The pressure field is obtained by applying the method of fundamental solutions which gives continuous function in the filter region. The components of filtration velocity are calculated from the appropriate derivatives. In numerical examples, various types of the filter are considered and some computational issues are discussed. A simple algorithm for achieving the optimal pseudo-boundary location is used, within the framework of the method of fundamental solutions, by minimizing the maximum absolute boundary error. Optimization results for various numbers of source points and collocation points are compared. The variation of total discharge with the inlet size is shown.

Keywords: filtration, Darcy equation, method of fundamental solutions, cylindrical fibrous filter

1. Introduction

Fibrous filters are one of the cost-effective means used to remove particulate matter suspended in gas stream. Most works on the filtration flow and collection efficiency have involved a single-fiber or microscopic point of view. This paper, by contrast, attempts to consider a filter as a whole. In order to calculate the collection efficiency, detailed information about a flow field in the filter is necessary. From the mathematical point of view, when modelling a filter as a porous medium, the pressure field or pressure squared field satisfies Laplace equation in the domain and mixed boundary conditions. Now, there are many numerical methods for solution of such a boundary value problem, e.g. FDM, FEM, FVM. However, these ones are mesh-based methods which means that the solution is given only at certain discrete points or is approximated by low-degree polynomials. In some cases, derivatives of the solution are most desirable.

During the last two decades, plenty of meshless methods have been developed and effectively applied to solve many problems in science and engineering. One of the techniques is the method of fundamental solutions (MFS), which provides an approximated solution being a continuous function with continuous derivatives. As yet, the MFS has been successfully applied to solve boundary value problems in a wide variety of disciplines. Most of authors consider planar domains which lead to particularly easy implementation of the meshless technique. However, in some cases spacial problems can be reduced to the two-dimensional ones. For instance, Karageorghis and Fairweather (1998, 1999, 2000) used the MFS to solve many axisymmetric problems in heat transfer, elasticity and acoustics. Also Ramachandran and Gunjal (2009) presented some axisymmetric heat transfer problems to compare various boundary collocation methods. As it was shown, the fundamental solution of the axisymmetric Laplace equation can be expressed in terms of complete elliptic integrals.

In our work, a problem of steady-state incompressible flow through a cylindrical filter is considered. As in many practical applications, it is assumed that the filter is filled with a fibrous porous medium and Darcy's law is employed to describe the phenomenon. The Laplace

type governing equation is solved by means of the MFS, which provides an approximation of the pressure field. Hence, it is easy to obtain velocity of the fluid flow and evaluate the total discharge. The knowledge of the filtration velocity field can be used for calculation of transport of contaminant particles, and their possible removal by the fibers can be investigated (e.g. see Dunnett and Clement, 2006). However, in this paper we restrict our study to determination of the velocity field only.

In this paper, the Darcy filtration equation is assumed to be the governing one. It is well known that this equation is justified for low Reynolds numbers. This condition is fulfilled in many cases of the filtration flow, because of low average flow velocity as well as small pore size. An extended discussion on applicability of Darcy's law can be found e.g. in the paper of Zeng and Grigg (2006). The authors revised two types of criteria, the Reynolds number and the Forchheimer number, and gave their critical values which relate to the situation when the so called 'non-Darcy effect' appears and hence Darcy's law stops being applicable.

An outline of this paper is as follows. In Section 2, we present mathematical description of the axisymmetric problem. Section 3 is devoted to the MFS formulation. In Section 4, we demonstrate some numerical experiments and discuss the results. Finally, conclusions and remarks are given in Section 5.

2. Mathematical formulation

2.1. Boundary value problem

Perhaps the simplest type of a cylindrical fibrous filter comprises a central inlet and outlet (see Fig. 1a). Let us consider the stationary fluid flow through such a filter whose internal geometry forms a cylinder of radius c and height h . Size of the inlet and outlet is specified by the radii a and b , respectively. Assume that the fluid is incompressible. It is exposed to the pressure p_{in} at the inlet and flows past the fibrous material within the filter. Finally, the outlet pressure equals p_{out} .

If we treat the fibrous material as an isotropic porous medium, then filtration velocity can be specified according to Darcy's law in terms of fluid pressure p

$$\mathbf{q} = -\frac{\kappa}{\mu} \text{grad } p \quad (2.1)$$

where κ is the permeability of the medium and μ is the dynamic viscosity of the fluid. Consequently, a continuity equation for the incompressible fluid reduces to Laplace's equation

$$\nabla^2 p = 0 \quad (2.2)$$

Due to axial symmetry of the problem, the potential p is independent of the angular coordinate φ . Thus, the domain can be reduced to a rectangular region Ω with boundary Γ whose revolution about the z -axis could form the original cylinder (see Fig. 1b). Now, governing equation (2.2) takes the form

$$\frac{\partial^2 p}{\partial r^2} + \frac{1}{r} \frac{\partial p}{\partial r} + \frac{\partial^2 p}{\partial z^2} = 0 \quad (2.3)$$

whereas the velocity vector has only two non-zero components

$$q_r = -\frac{\kappa}{\mu} \frac{\partial p}{\partial r} \quad q_z = -\frac{\kappa}{\mu} \frac{\partial p}{\partial z} \quad (2.4)$$

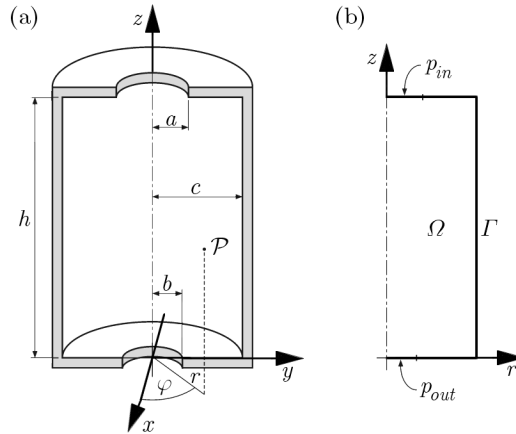


Fig. 1. Geometry of the filter: (a) 3-D cylindrical domain; the housing is filled with a fibrous porous medium, (b) the domain reduced to a rectangle

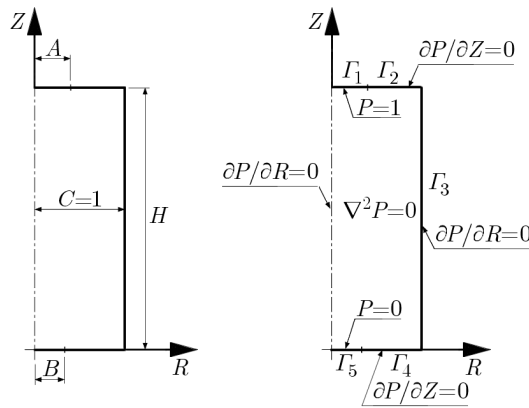


Fig. 2. Non-dimensional description of the domain and boundary conditions for the problem

Using c as a characteristic dimension, one can introduce the following non-dimensional variables (see Fig. 2)

$$R = \frac{r}{c} \quad Z = \frac{z}{c} \quad A = \frac{a}{c} \quad B = \frac{b}{c} \quad H = \frac{h}{c}$$

Moreover, the pressure p can be scaled according to the formula

$$P = \frac{p - p_{out}}{p_{in} - p_{out}}$$

so that $P_{in} = 1$ and $P_{out} = 0$. Now, for the dimensionless pressure field $P(R, Z)$, the velocity is given by

$$Q_R = \frac{c\mu}{\kappa\Delta p} q_r = -\frac{\partial P}{\partial R} \quad Q_Z = \frac{c\mu}{\kappa\Delta p} q_z = -\frac{\partial P}{\partial Z} \quad (2.5)$$

where $\Delta p = p_{in} - p_{out}$. Equation (2.3), in turn, can be rewritten in the following form

$$\frac{\partial^2 P}{\partial R^2} + \frac{1}{R} \frac{\partial P}{\partial R} + \frac{\partial^2 P}{\partial Z^2} = 0 \quad (2.6)$$

As it can be seen in Fig. 2, the boundary

$$\Gamma = \bigcup_{m=1}^5 \Gamma_m$$

and one can specify the boundary conditions as

$$\begin{aligned}
 P = f_1(R, Z) & \quad \text{on } \Gamma_1 & \quad \frac{\partial P}{\partial Z} = g_4(R, Z) & \quad \text{on } \Gamma_4 \\
 \frac{\partial P}{\partial Z} = g_2(R, Z) & \quad \text{on } \Gamma_2 & \quad P = f_5(R, Z) & \quad \text{on } \Gamma_5 \\
 \frac{\partial P}{\partial R} = g_3(R, Z) & \quad \text{on } \Gamma_3 & &
 \end{aligned} \tag{2.7}$$

where f_1 , f_5 and g_2 , g_3 , g_4 are prescribed functions for Dirichlet and Neumann boundary conditions, respectively. In the given case, we have $f_1 = 1$, $f_5 = 0$ and $g_2 = g_3 = g_4 = 0$. Additionally, the symmetry condition should be taken into consideration, that means zero derivative on the axis

$$\frac{\partial P}{\partial R} = 0 \quad \text{for } R = 0 \tag{2.8}$$

To sum up, in this axisymmetric problem we seek for the function $P(R, Z)$ which satisfies partial differential equation (2.6) in the domain Ω , together with conditions (2.7) on the boundary Γ and condition (2.8) on the axis.

2.2. Rate of fluid flow

After solving the problem, one can easily obtain the velocity field from Eq. (2.5) and evaluate the total discharge in the next step. It is sufficient to calculate the flow rate at the filter inlet

$$w = 2\pi \int_0^a q_z r \, dr \tag{2.9}$$

Hence

$$w = 2\pi c \frac{\kappa \Delta p}{\mu} \int_0^A Q_{ZR} \, dR = 2\pi c \frac{\kappa \Delta p}{\mu} W$$

where W is dimensionless discharge, which may be specified as

$$W = \int_0^A Q_{ZR} \, dR \tag{2.10}$$

When dealing with non-dimensional problem (2.6)-(2.8), the permeability of the porous medium is unimportant. However, its role is crucial in the calculation of dimensional velocity field and discharge evaluation. The permeability usually is expressed as some function of porosity of the fibrous medium times fibers diameter squared. Let us introduce the porosity term ε , which means a void fraction in the material. In literature the cell models proposed by Happel (1959) or Kuwabara (1959) and the improved ones by other authors (e.g. see Kołodziej *et al.*, 1998), are relatively popular. These models concern a two-dimensional arrangement of parallel fibers. In real media, a three-dimensional arrangement of fibers exists. Assuming that the arrangement of fibres is random and $0.4 \leq \varepsilon \leq 0.8$, one can use the experimental formula provided by Rahli *et al.* (1996)

$$\kappa = 0.0606 d_f^2 \frac{\pi \varepsilon^{5.1}}{4(1-\varepsilon)} \tag{2.11}$$

where d_f denotes the average fiber diameter.

3. Numerical solution procedure

Let us consider boundary value problem (2.6)-(2.8). If $\mathcal{P} = (R, Z)$ is a point in Ω , whereas the point $\mathcal{P}_j = (R_j, Z_j)$ does not belong to Ω , and

$$D^2 = (R + R_j)^2 + (Z - Z_j)^2 \quad k^2 = \frac{4RR_j}{D^2}$$

then the fundamental solution of axisymmetric Laplace equation (2.6) is given by

$$\Phi_j(R, Z) = \frac{4K(k)}{D} \tag{3.1}$$

and its partial derivatives are determined as

$$\begin{aligned} \frac{\partial \Phi_j}{\partial R} &= \frac{2\{D^2[E(k) - (1 - k^2)K(k)] - 2R(R + R_j)E(k)\}}{RD^3(1 - k^2)} \\ \frac{\partial \Phi_j}{\partial Z} &= -\frac{4(Z - Z_j)E(k)}{D^3(1 - k^2)} \end{aligned} \tag{3.2}$$

where $K(k)$ and $E(k)$ are the complete elliptic integrals of the first and second kind, respectively

$$K(k) = \int_0^{\pi/2} \frac{1}{\sqrt{1 - k^2 \sin^2 \theta}} d\theta \quad E(k) = \int_0^{\pi/2} \sqrt{1 - k^2 \sin^2 \theta} d\theta \tag{3.3}$$

In the MFS, the solution to the problem is approximated by a linear combination of the fundamental solutions Φ_j

$$P(R, Z) = \sum_{j=1}^N c_j \Phi_j(R, Z) \tag{3.4}$$

where c_j are unknown coefficients. The points $\{\mathcal{P}_j\}_{j=1}^N$ are singularities (or source points) located outside the solution domain. In practice, they are usually placed on some contour which is similar to the boundary Γ and lies at a distance S from Γ . Additionally, M collocation points \mathcal{P}_i are chosen on the boundary. Now, the coefficients c_j are determined in such a way that the boundary conditions are satisfied at the collocation points (Kolodziej and Zielinski, 2009, pp. 15-17). Fundamental solution (3.1) ensures the fulfillment of symmetry condition (2.8), thus we use the set of conditions (2.7) only

$$\begin{aligned} \sum_{j=1}^N c_j \Phi_j(R_i, Z_i) &= 1 && \text{for all } (R_i, Z_i) \in \Gamma_1 \\ \sum_{j=1}^N c_j \frac{\partial}{\partial Z} \Phi_j(R_i, Z_i) &= 0 && \text{for all } (R_i, Z_i) \in \Gamma_2 \\ \sum_{j=1}^N c_j \frac{\partial}{\partial R} \Phi_j(R_i, Z_i) &= 0 && \text{for all } (R_i, Z_i) \in \Gamma_3 \\ \sum_{j=1}^N c_j \frac{\partial}{\partial Z} \Phi_j(R_i, Z_i) &= 0 && \text{for all } (R_i, Z_i) \in \Gamma_4 \\ \sum_{j=1}^N c_j \Phi_j(R_i, Z_i) &= 0 && \text{for all } (R_i, Z_i) \in \Gamma_5 \end{aligned} \tag{3.5}$$

The number of the collocation points is given by

$$M = \sum_{m=1}^5 M_m$$

where M_m denotes the number of points on Γ_m . When $M = N$, linear algebraic system (3.5) can be solved with use of the Gauss elimination method. Otherwise, if $M > N$, the over-determined system is solved by the least squares approach. As values of the unknown coefficients are found, one can evaluate the pressure field from (3.4) and the velocity field according to (2.5) and (3.2).

4. Numerical experiments

4.1. Experiment 1

Now we turn to application of the presented solution procedure to a test problem. Consider a flow of water through a filter whose dimensions are specified as follows: $c = 40$ mm, $h = 140$ mm, $a = b = 10$ mm. Assume the inlet and outlet pressure: $p_{in} = 400$ kPa, $p_{out} = 200$ kPa. Moreover, for the porous material we take $\varepsilon = 0.6$ and $d_f = 0.15$ mm. The supposed viscosity of water is $\mu = 0.001$ Pa·s.

Firstly, we focus on determining the optimal placement of the source points. As mentioned above, they may lie on some pseudo-boundary, at the distance S from the boundary. In fact, the distance affects the solution accuracy, and choosing right values of S plays a key role in the MFS. According to the concept presented by Karageorghis (2009), we minimize the absolute maximum error e_{MAX} on Γ ; such a technique relies on the maximum principle for harmonic functions. Thus, we choose a set of M^* boundary points $\{(R_l, Z_l)\}_{l=1}^{M^*}$, different from the collocation points. Next, for consecutive values of S , we evaluate a difference between the solution (or its derivative) and the assumed boundary values

$$e_l = \begin{cases} P(R_l, Z_l) - f(R_l, Z_l) & \text{for Dirichlet boundary conditions} \\ \frac{\partial P}{\partial n}(R_l, Z_l) - g(R_l, Z_l) & \text{for Neumann boundary conditions} \end{cases}$$

where $\partial/\partial n$ denotes the outward normal derivative at the boundary point (R_l, Z_l) . Finally, the maximum absolute error is given by

$$e_{MAX} = \max_{l=1, \dots, M^*} |e_l| \quad (4.1)$$

Thus, one can find the optimal distance S_{opt} by minimization of the function $e_{MAX}(S)$. As can be seen in Fig. 3, in this problem, the objective function has a pseudo-random appearance beyond the initial range. Consequently, we use a simple search algorithm for the optimization, that means S is increased linearly to calculate the error.

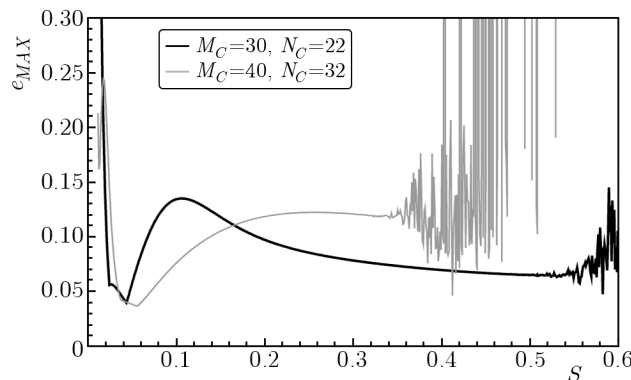


Fig. 3. Variation of the error with distance of source points

The analyzed results were obtained for various numbers M and N . However, two other symbols are used: M_C and N_C , which denote the numbers of collocation points and source

points per unit length C . On each boundary segment, the points are distributed proportionally and uniformly.

Figure 4 illustrates the maximum error when keeping M_C fixed and varying N_C . In each case, we searched for S_{opt} in the interval $\langle 0.01, 0.7 \rangle$ with a step $\Delta S = 0.001$. The graphs reveal that the improvement of the accuracy for increasing N_C is not so evident. Although the error is relatively high, it seems to stabilize for greater values of M_C within the approximate range $0.6 \leq N_C/M_C \leq 0.8$. Doubtless, the extreme case, when $N_C = M_C$, should be omitted.

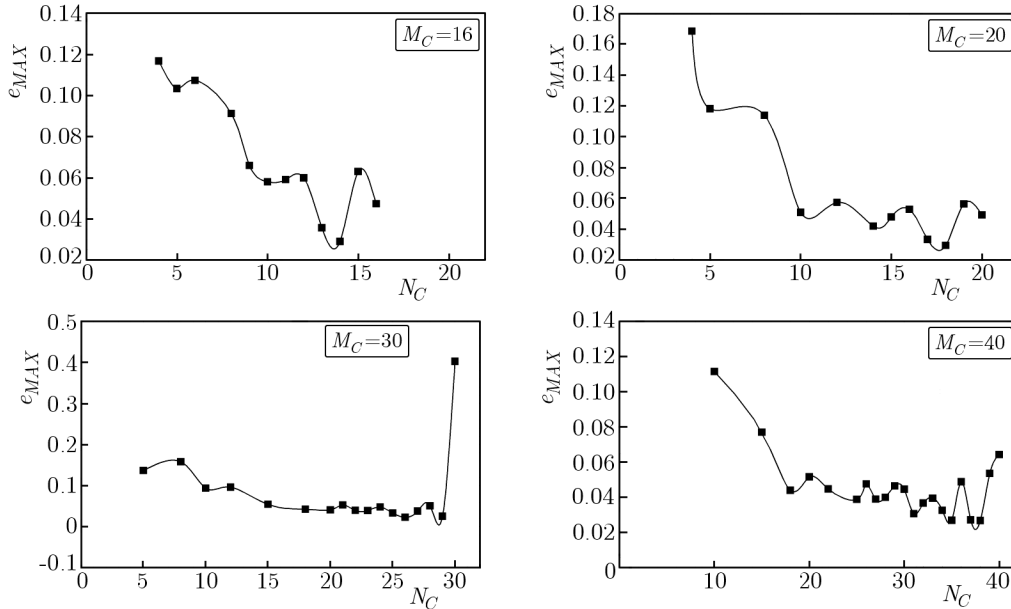


Fig. 4. Maximum error on the boundary

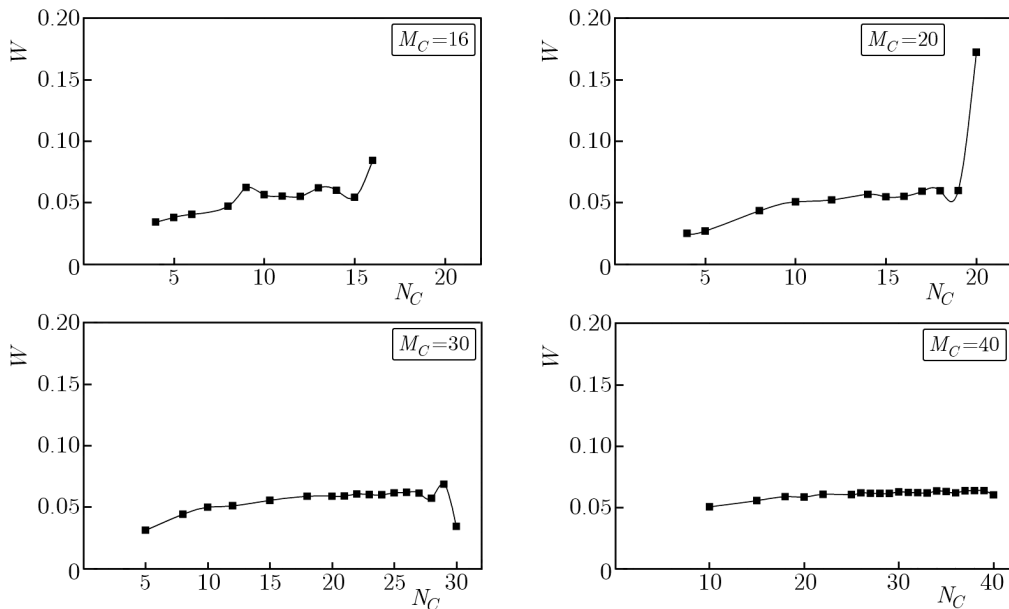


Fig. 5. Dimensionless total discharge

Actually, the key question is how the error impacts on values of the total discharge. The next four graphs (Fig. 5) show the non-dimensional quantity W for the given M_C and N_C . As with e_{MAX} , we observe similar intervals of N_C/M_C where very small fluctuations of the

discharge appear. It seems that the high error is local and does not disturb the velocity field considerably.

Table 1. Selected results of the error minimization

M_C	N_C	M	N	S_{opt}	e_{MAX}	e_{RMS}	W	w [l/min]	e_w
16	13	89	72	0.051	3.56E-02	1.06E-02	6.21E-02	37.048	2.51E-02
	14		78	0.075	2.90E-02	8.16E-03	6.02E-02	35.931	1.09E-02
20	14	111	78	0.074	4.20E-02	9.78E-03	6.05E-02	36.105	6.90E-03
	15		83	0.129	4.79E-02	9.98E-03	5.89E-02	35.126	6.60E-03
	16		89	0.393	5.28E-02	1.43E-02	5.95E-02	35.489	2.80E-03
	17		94	0.039	3.33E-02	9.51E-03	6.32E-02	37.693	3.03E-02
30	22	166	122	0.043	3.98E-02	7.61E-03	6.29E-02	37.549	1.04E-02
	23		127	0.065	3.93E-02	7.01E-03	6.18E-02	36.849	5.30E-03
	24		133	0.078	4.80E-02	8.12E-03	6.11E-02	36.462	1.80E-03
	25		138	0.026	3.32E-02	9.14E-03	6.39E-02	38.104	4.28E-02
	26		144	0.026	2.30E-02	7.38E-03	6.39E-02	38.121	1.28E-02
40	30	221	166	0.031	4.46E-02	6.91E-03	6.39E-02	38.095	1.04E-02
	31		171	0.040	3.07E-02	5.48E-03	6.31E-02	37.649	6.50E-03
	32		177	0.055	3.68E-02	5.58E-03	6.24E-02	37.257	2.60E-03
	33		182	0.019	3.95E-02	1.02E-02	6.42E-02	38.315	1.30E-03
	34		188	0.020	3.26E-02	7.48E-03	6.44E-02	38.401	1.20E-02
	35		193	0.035	2.70E-02	4.80E-03	6.33E-02	37.793	8.00E-03

Table 1 presents selected results of the discussed optimization. The examples show how the numbers M_C and N_C correspond to the total number of collocation and source points (M and N). Apart from the maximum absolute error, the root mean square one is given, according to the formula

$$e_{RMS} = \sqrt{\frac{1}{M^*} \sum_{l=1}^{M^*} e_l^2} \tag{4.2}$$

As it can be seen, the total discharge w , computed for the given dimensions and properties, fluctuates slightly and its approximate value is 37-38l/min. Additionally, the table includes values of the relative error between the total inflow and outflow. If the former quantity is treated as the reference one, the error can be expressed in the following way

$$e_w = \frac{|W_{out} - W_{in}|}{W_{in}} \tag{4.3}$$

where the subscripts “in” and “out” allow one to distinguish between the discharge at the filter inlet and outlet. As the results indicate, e_w does not exceed 5%, and in many cases is even less than 1%.

Figure 6, in turn, illustrates the distribution of the non-dimensional pressure and velocity in the Z direction obtained for $M_C = 40$, $N_C = 35$ and $S = S_{opt}$. Also, for the same parameters, we examined variation of the discharge W with the radius A assuming that B is constant (see Fig. 7). Obviously, the discharge value grows due to an increase of the inlet size.

As mentioned above, relatively high values of the boundary error seem to be a local effect. Indeed, the root mean square error is one order of magnitude smaller than the maximum absolute error (see Table 1). Presumably, the maximum values of the boundary error appear in the neighborhood of the so called boundary singularities: where the boundary condition suddenly changes from $P = f$ to $\partial P/\partial n = g$. For instance, Fig. 8 shows the error distribution on the

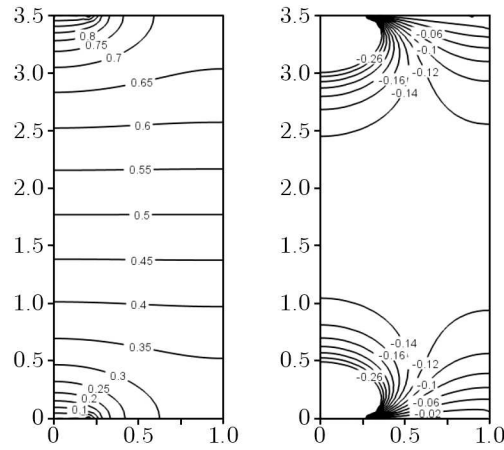


Fig. 6. Field of pressure (left) and Z -velocity (right) for $M_C = 40$, $N_C = 35$ and $S = S_{opt} = 0.035$

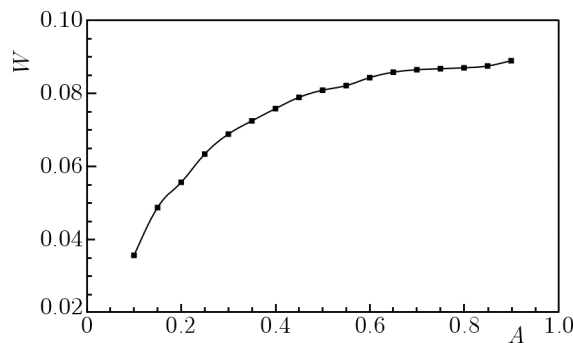


Fig. 7. Total discharge as a function of radius A

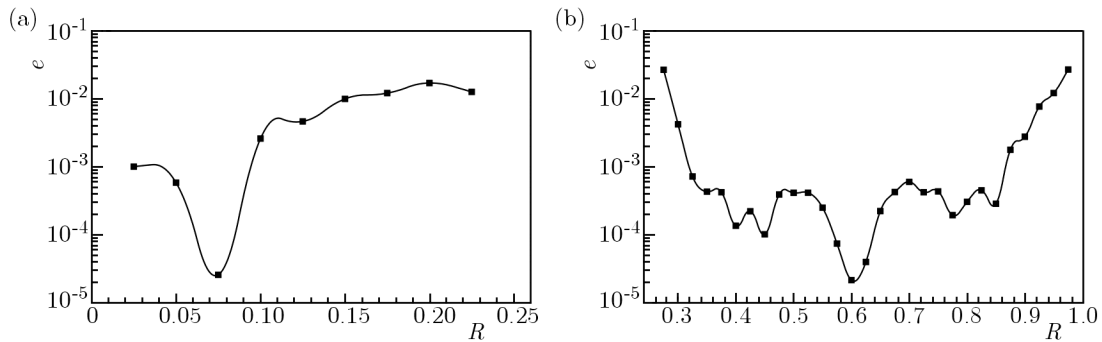


Fig. 8. Absolute error e on the upper boundary: (a) for $0 \leq R \leq A$; (b) for $A \leq R \leq C$

upper boundary ($Z = H$) of the filter: $\Gamma_1 \cup \Gamma_2$. The greatest values occur around the singularity for $R = A$. Moreover, a high error arises near by the corner ($R = C$).

4.2. Experiment 2

Let us now consider another type of cylindrical filter: assume that there is a circumferential outlet instead of the central one. We suppose that the filter housing, containing the fibrous material, is constructed in such a way that it does not disturb the axial symmetry of the fluid flow through the outlet.

The domain of such a problem is illustrated in Fig. 9. As can be seen, in this case, B denotes the outlet half-width. Also, the system of equations (3.5) should be slightly reformulated due to a change in boundary conditions (2.7)

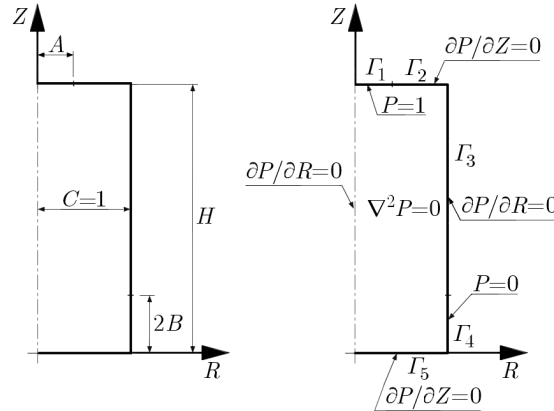


Fig. 9. The domain and boundary conditions for the filter with a circumferential outlet

$$\begin{aligned} \sum_{j=1}^N c_j \Phi_j(R_i, Z_i) &= 1 && \text{for all } (R_i, Z_i) \in \Gamma_1 \\ \sum_{j=1}^N c_j \frac{\partial}{\partial Z} \Phi_j(R_i, Z_i) &= 0 && \text{for all } (R_i, Z_i) \in \Gamma_2 \\ \sum_{j=1}^N c_j \frac{\partial}{\partial R} \Phi_j(R_i, Z_i) &= 0 && \text{for all } (R_i, Z_i) \in \Gamma_3 \\ \sum_{j=1}^N c_j \Phi_j(R_i, Z_i) &= 0 && \text{for all } (R_i, Z_i) \in \Gamma_4 \\ \sum_{j=1}^N c_j \frac{\partial}{\partial Z} \Phi_j(R_i, Z_i) &= 0 && \text{for all } (R_i, Z_i) \in \Gamma_5 \end{aligned}$$

For computations, assume the following dimensions: $c = 45$ mm, $h = 200$ mm, $a = 15$ mm, $b = 20$ mm. Moreover, we take $p_{in} = 400$ kPa, $p_{out} = 250$ kPa and $\mu = 0.001$ Pa·s. For the porous material $\varepsilon = 0.6$ and $d_f = 0.15$ mm.

Similarly to the first experiment, we applied the optimization algorithm for various values of M_C and N_C , when $S \in \langle 0.01, 0.7 \rangle$ and $\Delta S = 0.001$. Table 2 presents selected results. Accordingly, the total discharge w is approximately equal to 48 l/min. Again, its fluctuations comes from locally high boundary error, particularly near the singularity at $R = A$. The minimization procedure allows one to reduce e_{MAX} below 3%. The discharge error, e_W in turn, reaches 1-2%; only for the lowest M_C the error is greater than 5%.

Table 2. Selected results of the error minimization

M_C	N_C	M	N	S_{opt}	e_{MAX}	e_{RMS}	W	w [l/min]	e_W
16	13	104	84	0.051	2.90E-02	8.01E-03	9.36E-02	47.125	1.68E-02
	14		91	0.089	3.95E-02	7.46E-03	9.08E-02	45.712	5.49E-02
20	16	130	104	0.038	3.18E-02	9.55E-03	9.50E-02	47.811	2.10E-03
	17		110	0.058	3.30E-02	6.82E-03	9.30E-02	46.823	1.85E-02
30	23	194	149	0.051	3.16E-02	5.06E-03	9.48E-02	47.698	9.10E-03
	25		162	0.027	3.66E-02	7.24E-03	9.62E-02	48.434	5.80E-03
	26		168	0.026	2.87E-02	6.95E-03	9.60E-02	48.303	1.19E-02
40	30	259	194	0.064	3.78E-02	4.05E-03	9.47E-02	47.678	1.52E-02
	34		220	0.020	3.24E-02	6.64E-03	9.66E-02	48.619	5.10E-03
	35		226	0.020	2.70E-02	6.11E-03	9.69E-02	48.777	1.87E-02

Figure 10 shows distribution of the non-dimensional pressure and axial velocity computed for $M_C = 40$, $N_C = 35$ and $S = S_{opt}$. The change with the radius A in the discharge W has the same character as before (see Fig. 11).

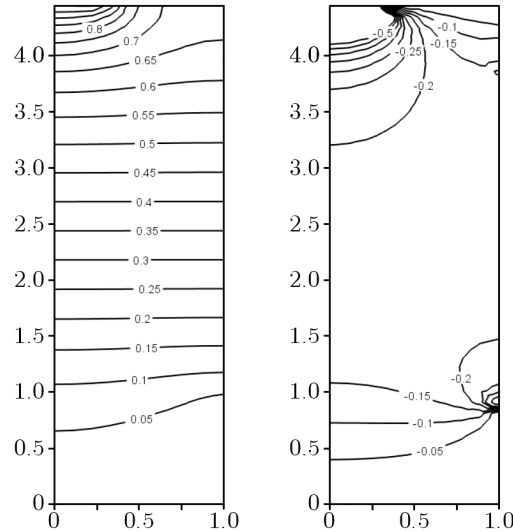


Fig. 10. Field of pressure (left) and Z -velocity (right) for $M_C = 40$, $N_C = 35$ and $S = S_{opt} = 0.02$

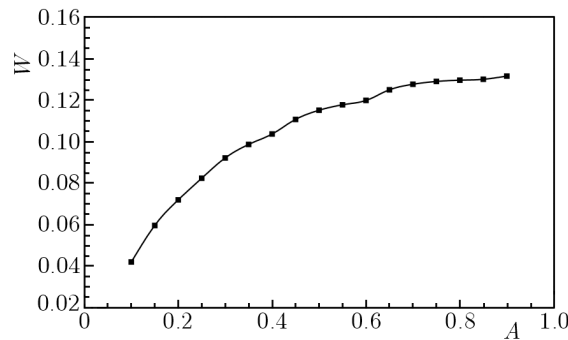


Fig. 11. Total discharge as a function of radius A

4.3. Experiment 3

Finally, consider a filter with both circumferential inlet and outlet. Herein, one should also assume that the structure of the filter housing does not disturb the radial flow through such an inlet and outlet. The resulting domain of the filtration problem is presented in Fig. 12. Here, B denotes the outlet half-width, whereas A is the inlet half-width. Because of the different geometry, the system of equations (3.5) takes the form

$$\begin{aligned}
 \sum_{j=1}^N c_j \frac{\partial}{\partial Z} \Phi_j(R_i, Z_i) &= 0 && \text{for all } (R_i, Z_i) \in \Gamma_1 \\
 \sum_{j=1}^N c_j \Phi_j(R_i, Z_i) &= 1 && \text{for all } (R_i, Z_i) \in \Gamma_2 \\
 \sum_{j=1}^N c_j \frac{\partial}{\partial R} \Phi_j(R_i, Z_i) &= 0 && \text{for all } (R_i, Z_i) \in \Gamma_3 \\
 \sum_{j=1}^N c_j \Phi_j(R_i, Z_i) &= 0 && \text{for all } (R_i, Z_i) \in \Gamma_4 \\
 \sum_{j=1}^N c_j \frac{\partial}{\partial Z} \Phi_j(R_i, Z_i) &= 0 && \text{for all } (R_i, Z_i) \in \Gamma_5
 \end{aligned}$$

What is more, the formulas related to the total discharge must be modified. For the circumferential inlet we have

$$w = 2\pi c \int_{h-2a}^h q_r dz = 2\pi c \frac{\kappa \Delta p}{\mu} \int_{H-2A}^H Q_R dZ = 2\pi c \frac{\kappa \Delta p}{\mu} W \quad (4.4)$$

where the dimensionless discharge W is given by

$$W = \int_{H-2A}^H Q_R dZ \quad (4.5)$$

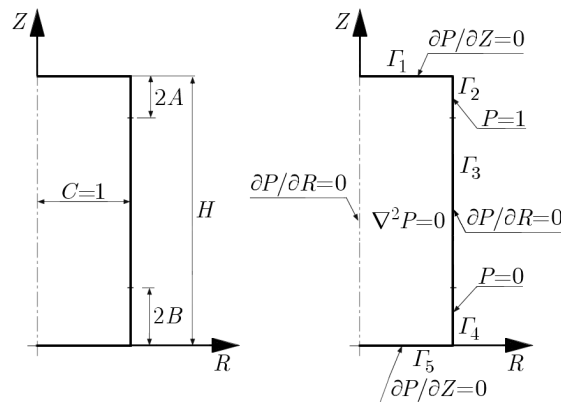


Fig. 12. The domain and boundary conditions for the filter with a circumferential outlet

In this example, suppose the dimensions: $c = 45$ mm, $h = 200$ mm, $a = 25$ mm, $b = 20$ mm. Moreover, assume that $p_{in} = 400$ kPa, $p_{out} = 200$ kPa, $\mu = 0.001$ Pa·s, $\varepsilon = 0.5$ and $d_f = 0.15$ mm.

The making use of the optimization procedure ($S \in \langle 0.01, 0.7 \rangle$ and $\Delta S = 0.001$) produced the results shown in Table 3. As can be seen, the dimensional discharge $w \approx 35$ l/min. In this case, the highest values of the boundary error occur at two singular points: at $Z = 0$ and $Z = H$ as $R = C$. Taking $S = S_{opt}$ can reduce the maximum error below 2%. Furthermore, it should be noticed that the error e_W reaches smaller values than in the two previous experiments.

Table 3. Selected results of the error minimization

M_C	N_C	M	N	S_{opt}	e_{MAX}	e_{RMS}	W	w [l/min]	e_W
16	13	105	84	0.493	1.96E-02	4.72E-03	1.64E-01	34.662	4.00E-03
	14		91	0.477	1.87E-02	6.06E-03	1.66E-01	35.217	1.00E-04
20	14	130	91	0.443	1.87E-02	5.24E-03	1.64E-01	34.763	2.90E-03
	15		97	0.466	1.72E-02	4.68E-03	1.65E-01	34.846	1.04E-02
30	22	195	142	0.321	1.70E-02	3.74E-03	1.66E-01	35.260	3.00E-04
	23		149	0.275	1.49E-02	4.64E-03	1.66E-01	35.153	3.00E-03
	24		155	0.306	1.64E-02	4.17E-03	1.66E-01	35.254	7.80E-03
40	31	259	200	0.207	1.75E-02	3.75E-03	1.66E-01	35.217	1.60E-03
	32		207	0.200	1.74E-02	3.44E-03	1.65E-01	34.956	3.20E-03
	34		220	0.201	1.52E-02	3.12E-03	1.66E-01	35.126	6.40E-03

The distribution of the pressure P and the velocity Q_Z is presented in Fig. 13. The $W(A)$ function, in turn, is shown in Fig. 14. One can observe that the dependency is of different nature for the circumferential inlet and outlet.

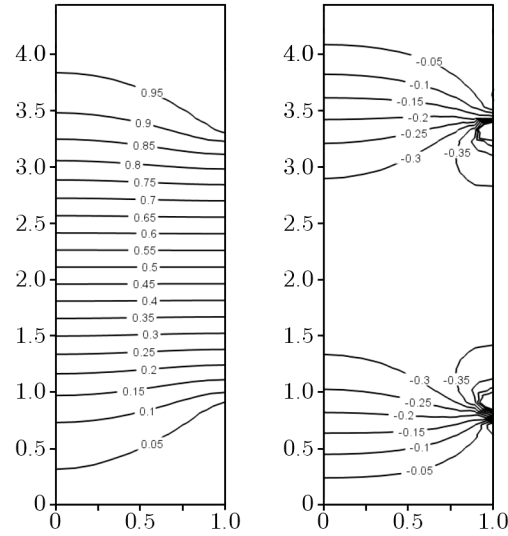


Fig. 13. Field of pressure (left) and Z -velocity (right) for $M_C = 40$, $N_C = 32$ and $S = S_{opt} = 0.2$

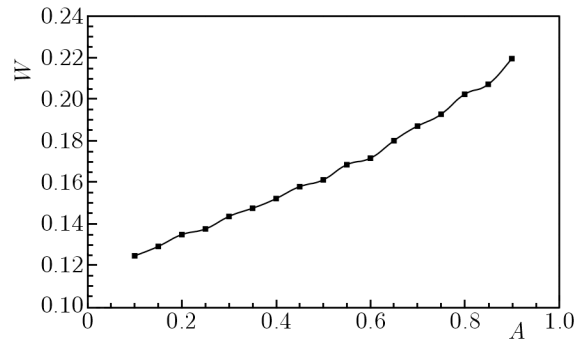


Fig. 14. Total discharge as a function of radius A

5. Final remarks

In this work, we have presented the application of the method of fundamental solutions to steady-state fluid flow through a cylindrical filter. Due to axial symmetry of the domain and boundary conditions, the problem has been reduced to a two-dimensional one. This formulation has led to very easy implementation of the method, which should be emphasized.

In this paper, we assumed that the fluid is incompressible. For a gas flow through a filter, one can take into account the compressibility. The continuity equation for a steady axisymmetric compressible flow has the form

$$\frac{1}{r} \frac{\partial}{\partial r} (r \rho q_r) + \frac{\partial}{\partial z} (\rho q_z) = 0 \tag{5.1}$$

where ρ is density. According to the equation of state for the perfect gas $\rho = p/(RT)$ and Darcy's law for isothermal condition, the continuity equation takes the form

$$\frac{1}{r} \frac{\partial}{\partial r} \left(r p \frac{\partial p}{\partial r} \right) + \frac{\partial}{\partial z} \left(p \frac{\partial p}{\partial z} \right) = 0 \tag{5.2}$$

or the equivalent form

$$\frac{1}{r} \frac{\partial}{\partial r} \left(r \frac{\partial p^2}{\partial r} \right) + \frac{\partial}{\partial z} \left(\frac{\partial p^2}{\partial z} \right) = 0 \tag{5.3}$$

The last equation has the same form as equation (2.3), if instead of pressure p , we have pressure squared p^2 . This equation must be solved with the same boundary conditions as for the incompressible flow (see e.g. Uściłowska and Kołodziej, 2006). In such a case, the methodology of solution of the nondimensional problem is practically the same as for the incompressible case. Differences essentially exist in calculation of dimensional parameters.

The presented numerical examples have been related to various types of the cylindrical filter: diverse positions of the inlet and outlet have been considered. In all the cases, we used a simple algorithm for achieving the optimal pseudo-boundary location by minimizing the maximum absolute boundary error. The optimization results for various number of source points and collocation points have been compared. In our experiments, the maximum error is relatively high, however, it turns out that it does not significantly affect the pressure and velocity distribution. As it has been shown, the maximum error appears in the neighborhood of the boundary singularities, due to a sudden change in boundary conditions.

Since a non-zero difference between total inflow and outflow is a purely numerical effect, it can be also treated as a measure of the solution quality. The obtained results indicate that in most cases the discharge error is lower than 2% and has the smallest values as both the inlet and outlet of the filter are circumferential.

Moreover, we examined the variation of total discharge with the inlet size. The function is qualitatively different when dealing with the filter comprising a circumferential inlet and outlet.

All in all, with the typical advantages of the meshless methods (e.g. no discretization of the domain), the method of fundamental solutions allows one to obtain reasonable results: the field of pressure and velocity as well as the total discharge within acceptable tolerance.

References

1. DUNNETT S.J., CLEMENT C.F., 2006, A numerical study of the effects of loading from diffusive deposition on the efficiency of fibrous filters, *Aerosol Science*, **37**, 1116-1139
2. HAPPEL J., 1959, Viscous flow relative to arrays of cylinders, *AIChE Journal*, **5**, 174-177
3. KARAGEORGHIS A., 2009, A Practical Algorithm for Determining the Optimal Pseudo-Boundary in the Method of Fundamental Solutions, *Advances in Applied Mathematics and Mechanics*, **1**, 510-528
4. KARAGEORGHIS A., FAIRWEATHER G., 1998, The method of fundamental solutions for axisymmetric acoustic scattering and radiation problems, *Journal Acoustical Society of America*, **104**, 3212-3218
5. KARAGEORGHIS A., FAIRWEATHER G., 1999, The Method of Fundamental Solutions for axisymmetric potential problems, *International Journal for Numerical Methods in Engineering*, **44**, 1653-1669
6. KARAGEORGHIS A., FAIRWEATHER G., 2000, The Method of Fundamental Solutions for axisymmetric elasticity problems, *Computational Mechanics*, **25**, 524-532
7. KOŁODZIEJ J.A., DZIĘCIELAK R., KOŃCZAK Z., 1998, Permeability tensor for heterogeneous porous medium of fibrous type, *Transport in Porous Media*, **32**, 1-19
8. KOŁODZIEJ J.A., ZIELINSKI A.P., 2009, *Boundary Collocation Techniques and their Application in Engineering*, WIT Press, Southampton
9. KUWABARA S., 1959, The forces experienced by randomly distributed parallel circular cylinders or spheres in viscous flow at small Reynolds numbers, *Journal of Physical Society of Japan*, **14**, 527-532
10. RAHLI O., TADRIST L., MISCEVIC M., 1996, Experimental analysis of fibrous porous media permeability, *AIChE Journal*, **42**, 3547-3549

11. RAMACHANDRAN P.A., GUNJAL P.R., 2009, Comparison of boundary collocation methods for singular and non-singular axisymmetric heat transfer problems, *Engineering Analysis with Boundary Elements*, **33**, 704-716
12. UŚCIŁOWSKA A., KOŁODZIEJ J.A., 2006, Solution of the nonlinear equation for isothermal gas flows in porous medium by Trefftz method, *Computer Assisted Mechanics and Engineering Science*, **13**, 445-456
13. ZENG Z-W., GRIGG R., 2006, A criterion for non-Darcy flow in porous media, *Transport in Porous Media*, **63**, 57-69

Manuscript received September 23, 2011; accepted for print November 8, 2013